Bioinspired superhydrophobic, self-cleaning and low drag surfaces

Bharat Bhushan[1]

Ohio Eminent Scholar and Howard D. Winbigler Professor
Director, Nanoprobe Laboratory for Bio- & Nanotechnology and Biomimetics
W390 Scott Laboratory
The Ohio State University, Columbus, OH 43210-1142, USA

ABSTRACT

Nature has evolved objects with desired functionality using commonly found materials. Nature capitalizes on hierarchical structures to achieve functionality. The understanding of the functions provided by objects and processes found in nature can guide us to produce nanomaterials, nanodevices, and processes with desirable functionality. This article provides an overview of four topics: (1) Lotus Effect used to develop superhydrophobic and self-cleaning/anti-fouling surfaces with low adhesion, (2) Shark Skin Effect to develop surfaces with low fluid drag and anti-fouling characteristics, and (3-4) Rice Leaf and Butterfly Wing Effect to develop superhydrophobic and self-cleaning surfaces with low drag. Rice Leaf and Butterfly Wings combine the Shark Skin and Lotus Effects.

1. INTRODUCTION

Nature has gone through evolution over the 3.8 billion years, since life is estimated to have appeared on earth. Nature has evolved objects with desired functionality using commonly found materials. These function on the macroscale to the molecular scale. The understanding of the functions provided by objects and processes found in nature can guide us to produce nanomaterials, nanodevices, and processes with desirable functionality. Biologically inspired design or adaptation or derivation from nature is referred to as "biomimetics." It means mimicking biology or nature. Biomimetics is derived from the Greek word biomimesis. Other words used include bionics, biomimicry, and biognosis. The field of biomimetics is highly interdisciplinary. It involves the understanding of biological functions, structures, and principles of various objects found in nature by biologists, physicists, chemists, and material scientists and the design and fabrication of various materials and devices of commercial interest from bioinspiration.

Biological materials are highly organized from the molecular scale to the nanoscale, microscale, and macroscale, often in a hierarchical manner with intricate nanoarchitecture that ultimately makes up a myriad of different functional elements. Nature uses commonly found materials. The properties of the materials and surfaces result from a complex interplay between the surface structure and the morphology and physical and chemical properties. Many materials, surfaces, and devices provide multifunctionality. Molecular scale devices, superhydrophobicity, self-cleaning,

[1] Email: bhushan.2@osu.edu

Nanostructured Thin Films VI, edited by Tom G. Mackay, Akhlesh Lakhtakia, Yi-Jun Jen, Motofumi Suzuki,
Proc. of SPIE Vol. 8818, 881802 · © 2013 SPIE · CCC code: 0277-786X/13/$18 · doi: 10.1117/12.2025150

drag reduction in fluid flow, antifouling, energy conversion and conservation, reversible adhesion, aerodynamic lift, materials and fibers with high mechanical strength, biological self-assembly, anti-reflection, structural coloration, thermal insulation, self-healing, and sensory aid mechanisms are some of the examples found in nature which are of commercial interest[1-3].

Various features found in natural objects are on the nanoscale. The major emphasis on nanoscience and nanotechnology since the early 1990s has provided a significant impetus in mimicking nature using nanofabrication techniques for commercial applications. Biomimetics has spurred interest across many disciplines. Various biomimetics-inspired materials and objects are being fabricated in labs around the world, and some have found industrial applications.

In this invited keynote article, an overview of four of the topics shown in **Fig. 1** is provided: (1) Lotus Effect used to develop superhydrophobic and self-cleaning/anti-fouling surfaces with low adhesion, (2) Shark Skin Effect to develop surfaces with low fluid drag and anti-fouling characteristics, and (3-4) Rice Leaf and Butterfly Wing Effect to develop superhydrophobic and self-cleaning surfaces with low drag. Rice Leaf and Butterfly Wings combine the Shark Skin and Lotus Effects.

2.0 LOTUS EFFECT

Superhydrophobic surfaces with a high static contact angle above 150º and contact angle hysteresis (the difference between the advancing and receding contact angles) of less than 10º exhibit extreme water repellence and self-cleaning properties[4]. At a low value of contact angle hysteresis, water droplets may roll in addition to slide, which facilitates the removal of contaminant particles. Surfaces with low contact angle hysteresis have a low water roll-off (tilt) angle, which denotes the angle to which a surface must be tilted for water droplets to roll off. Superhydrophobic and self-cleaning surfaces are of interest for various applications including self-cleaning windows, windshields, exterior paints for buildings and navigation of ships, utensils, roof tiles, textiles, solar panels, and applications requiring a reduction of drag in fluid flow, e.g., in micro/nanochannels. They also exhibit antifouling which is of interest such as in membranes used for desalination and water purification. These surfaces can also be used for energy conversion and energy conservation. Condensation of water vapor from the environment and/or process liquid film can form menisci, leading to high adhesion in devices requiring relative motion[5]. Superhydrophobic surfaces are needed to minimize adhesion between a surface and a liquid.

A model surface for superhydrophobicity and self-cleaning is provided by the leaves of the Lotus plant (*Nelumbo nucifera*) (**Fig. 1**, top left) [2, 6, 7]. The leaf surface is very rough due to so-called papillose epidermal cells, which form asperities or papillae. In addition to the microscale roughness the surface of the papillae is also rough with sub-micron sized asperities composed of 3-D epicuticular waxes. The waxes of the Lotus are tubules, but on other leaves waxes also exist in form of platelets or other morphologies. Lotus leaves have hierarchical structures, which have been

studied by Bhushan and Jung[8]. The water droplets on these surfaces readily sit on the apex of the nanostructures because air bubbles fill the valleys of the structure under the droplet. Therefore, these leaves exhibit considerable superhydrophobicity. The water droplets on the leaf surfaces remove any contaminant particles present when they roll off, leading to self-cleaning. It has been reported that nearly all superhydrophobic and self-cleaning leaves consist of an intrinsic hierarchical structure[7]. Water on such a surface forms a spherical droplet, and both the contact area and the adhesion to the surface are dramatically reduced[4].

Based on the so-called Lotus effect, one of the ways to increase the hydrophobic property of the surface is to increase surface roughness, so roughness-induced hydrophobicity has become a subject of extensive investigations. Wenzel[9] suggested a simple model predicting that the contact angle of a liquid with a rough surface is different from that with a smooth surface. Cassie and Baxter[10] showed that a gaseous phase including water vapor, commonly referred to as "air" in the literature, may be trapped in the cavities of a rough surface, resulting in a composite solid-liquid-air interface, as opposed to the homogeneous solid-liquid interface. These two models describe two possible wetting regimes or states: the homogeneous (Wenzel) and the composite (Cassie-Baxter) regimes.

The formation of a composite interface is a multiscale phenomenon which depends upon the relative sizes of the liquid droplet and roughness details. A composite interface is metastable, and its stability is an important issue. Even though it may be geometrically possible for the system to become composite, it may be energetically profitable for the liquid to penetrate into the valleys between asperities and form the homogeneous interface. The composite interface is fragile and can be irreversibly transformed into the homogeneous interface, thus damaging superhydrophobicity. Many authors have investigated the stability of artificial superhydrophobic surfaces and showed that whether the interface is homogeneous or composite may depend on the history of the system, in particular whether the liquid was applied from the top or condensed at the bottom. Nosonovsky and Bhushan[4] have identified mechanisms which lead to the destabilization of the composite interface, namely, the capillary waves, condensation and accumulation of nanodroplets, and surface inhomogeneity. They also reported that a convex surface leads to a stable interface and high contact angle. They have suggested the effects of a droplet's weight and curvature among the factors which affect the transition. It has been demonstrated that a combination of microroughness and nanoroughness (multiscale roughness) with convex surfaces can help to resist destabilization by pinning the interface. High asperities resist the capillary waves, while nanobumps prevent nanodroplets from filing the valleys between asperities and pin them. The effect of roughness on wetting is scale dependent, and mechanisms that lead to the destabilization of a composite interface are also scale-dependent. To effectively resist these scale-dependent mechanisms, it is expected that a multiscale roughness (such as a hierarchical structure) is optimum for superhydrophobicity.

For stability of a composite interface, a schematic structure of an easily-manufacturable hierarchical surface is shown in **Fig. 2**. The asperities should be high enough so that the droplet does not touch the valleys.

2.1 Fabrication and characterization of micro- , nano- and hierarchical structured surfaces

In this section, we describe measurements of the wetting properties of micro-, nano- and hierarchical structured surfaces fabricated using different techniques. Various attempts have been made to fabricate mechanically durable structures using multi-walled carbon nanotube (CNT) arrays with high mechanical strength. A simpler approach is to use CNT composites. CNT composites were deposited on flat epoxy resin and a microstructure to create nano- and hierarchical structures using a spray method. Jung and Bhushan[11] measured the static contact angle and contact angle hysteresis on nano- and hierarchical structures with CNT. For static contact angle and contact angle hysteresis, after introducing the CNT nanostructure on top of the micropatterned Si replica, a high static contact angle of 170° and low contact angle hysteresis of 2° were found for the hierarchical structures. Both nano- and hierarchical structures created with CNT showed superhydrophobicity and self-cleaning ability.

To investigate the durability of the nanostructure fabricated using CNT, Jung and Bhushan[11] conducted wear tests by creating wear scars with a 15 μm radius borosilicate ball using an AFM for 1 cycle at two normal loads of 100 nN and 10 μN using AFM. **Figure 3** shows surface height maps before and after wear tests for nanostructures with CNT. As the normal load of 100 nN was applied on the nanostructure with CNT, the wear scar induced on the surface was not found or could not be measured. It was also hard to quantify a wear depth on the nanostructure with CNT scanned with a borosilicate ball. With increasing the normal load to 10 μN, it was found that the wear depth on the nanostructure with CNT was not significantly changed, but the morphology of the CNT differed slightly from that before the wear test. It can be interpreted that the individual CNT might be expected to slide or bend by the borosilicate ball applied by high normal load of 10 μN during the test process.

Ebert and Bhushan[12, 13] used a mixture of microscale and nanoscale SiO_2 particles to create hierarchical structure patterns on flat epoxy substrates. In addition, hierarchical structure was created by depositing nanoscale SiO_2, ZnO, and ITO particles onto micropatterned epoxy substrates to create optically transparent surfaces. The data showed that the structures are superhydrophobic and self-cleaning with low adhesion and high mechanical durability.

2.2 Summary

To develop Lotus-inspired mechanical durable surfaces, CNT-composite and micro- and nanoparticle composite hierarchical structures have been fabricated. They exhibit high durability for industrial applications.

3.0 SHARK SKIN EFFECT

Nature has created ways of reducing drag in fluid flow, evident in the efficient movement of fish, dolphins, and sharks. The mucus secreted by fish causes a reduction in drag as they move through water, and also protects the fish from abrasion by making the fish slide across objects rather than scrape and disease by making the surface of the fish difficult for microscopic organisms to adhere to. It has been known for many years that by adding as little as a few hundred parts per million guar, a naturally occurring polymer, friction in pipe flow can be reduced by up to two-thirds.

The compliant skin of the dolphin has also been studied for drag reducing properties. By responding to the pressure fluctuations across the surface, a compliant material on the surface of an object in a fluid flow has been shown to be beneficial. Though early studies showed dramatic drag reduction benefits, later studies have only been able to confirm 7% drag reduction[14].

Another set of aquatic animals which possesses multi-purpose skin is fast swimming sharks. The skin of fast swimming sharks protects against biofouling and reduces the drag experienced by sharks as they swim through water[15]. The tiny scales covering the skin of fast swimming sharks, known as dermal denticles (skin teeth), are shaped like small riblets and aligned in the direction of fluid flow (**Fig. 1**, top right). Shark skin inspired riblets have been shown to provide a drag reduction benefit up to 9.9% [16]. The spacing between these dermal denticles is such that microscopic aquatic organisms have difficulty adhering to the surface. Slower sharks are covered in dermal denticles as well, but not those which are shaped like riblets or provide any drag reduction benefit.

Fully developed turbulent flow is commonly said to exhibit complete randomness in its velocity distribution, but there exist distinct regions within fully developed turbulent flow that exhibit different patterns and flow characteristics[17]. While organization is evident in the viscous sublayer, the layer closest to the surface, the outer layers of the turbulent boundary layer are chaotic and disorganized. Much of this chaotic motion above the viscous sublayer is caused by the outward bursting of the streamwise vortices that form at the surface in the viscous sublayer. Streamwise vortices (vortices which rotate about axes in the direction of mean velocity) dominate the viscous sublayer. As these vortices rotate and flow along the surface, they naturally translate across the surface in the cross-flow direction. The interaction between the vortices and the surface, as well as between neighboring vortices that collide during translation initiate bursting motions where vortices are rapidly ejected from the surface and into the outer boundary layers. As vortices are ejected, they tangle with other vortices and twist such that transient velocity vectors in the cross-stream direction can become as large as those in the average flow direction. The translation, bursting of vortices out of the viscous sublayer, and chaotic flow in the outer layers of the turbulent boundary layer flow are all forms of momentum transfer and are large factors in fluid drag. Reducing the bursting behavior of the streamwise vortices is a critical goal of drag reduction, as the drag reduction possibilities presented by this are sizable.

The small riblets that cover the skin of fast swimming sharks work by impeding the cross-stream translation of the streamwise vortices in the viscous sublayer. The mechanism by which the riblets interact with and impede vortex translation is complex, and the entirety of the phenomena is not yet fully understood. On a practical level, impeding the translation of vortices reduces the occurrence of vortex ejection into the outer boundary layers as well as the momentum transfer caused by tangling and twisting of vortices in the outer boundary layers.

In the turbulent flow regime, fluid drag typically increases dramatically with an increase in surface area due to the shear stresses at the surface acting across the new, larger surface area. However, as vortices form above a riblet

surface, they remain above the riblets, interacting with the tips only and rarely causing any high-velocity flow in the valleys of the riblets. Since the higher velocity vortices interact only with a small surface area at the riblet tips, only this localized area experiences high shear stresses. The low velocity fluid flow in the valleys of the riblets produces very low shear stresses across the majority of the surface of the riblet. By keeping the vortices above the riblet tips, the cross-stream velocity fluctuations inside the riblet valleys are much lower than the cross-stream velocity fluctuations above a flat plate[18]. This difference in cross-stream velocity fluctuations is evidence of a reduction in shear stress and momentum transfer near the surface, which minimizes the effect of the increased surface area.

3.1 Optimization of riblet geometry

Most studies are done by changing the non-dimensionalized riblet spacing, s^+, by varying only fluid velocity and collecting shear stress data from a shear stress balance in a wind tunnel or open flow channel with oil and water. Measured shear stress is compared to shear stress over a flat plate and plotted against the calculated s^+ value for the flow conditions. In this manner, a performance curve is created for a riblet array with a specific set of characteristic dimensions. The use of nondimensional characteristic dimensions for riblet studies, namely nondimensional spacing, s^+, is important for comparison between studies performed under different flow conditions. Non-dimensionalization accounts for the change in size of flow structures like vortex diameter, which is the critical value to which riblets must be matched. Experiments have been carried out with various types of riblets, surface materials and in air, oil, and water[16, 19, 20]. Under the same non-dimensionalized flow conditions, riblet arrays sharing characteristic dimension ratios create similar performance curves whether they are made of different materials, are tested in different fluids, or fabricated at a different scale.

Sawtooth, scalloped, and blade riblets have been studied. When comparing the optimal drag reduction geometries for sawtooth, scalloped, and blade riblets, blade riblets provide the highest level of drag reduction, scalloped riblets provide the second most, and sawtooth riblets provide the least benefit.

More recently there have been studies which have investigated the drag reduction properties of riblet-topped shark scales as both a static structure[21]and a flexible—possibly controllable—member[22]. Using the scales molded in epoxy resin from the skin of the Spiny Dogfish (Squalus acanthias), shown in **Fig. 4a**, Jung and Bhushan[21] have reported a decrease in pressure drop—corresponding to a decrease in fluid drag—versus a smooth surface in a rectangular flow cell experiment. Pressure drop from inlet to outlet of a channel is a measure of drag with a large pressure drop occurring as a result of high drag (**Fig. 4b**). In addition, some decrease in pressure drop was realized in a similar experiment using segmented aligned riblets fabricated on acrylic compared to a smooth acrylic test section (**Fig. 4b**).

Bixler and Bhushan[23-25] fabricated blade type continuous riblets with various geometrical dimensions on acrylic sheets using laser etching. They made pressure drop measurements in rectangular flow cell incorporating the riblets in

water, air, and oil fluids. They also performed wind tunnel experiments on vinyl sheets with continuous sawtooth riblets. In all cases, they reported that riblets showed pressure drop reduction in turbulent flow.

3.2 Application of riblets for drag reduction

The dominant and perhaps only commercial market where riblet technology for drag reduction is commercially sold is competitive swimwear. The general population became aware of shark skin's drag reduction benefits with the introduction of the FastSkin® suits by Speedo in 2004. Speedo claimed a drag reduction of several percent in a static test compared to other race suits. However, given the compromises of riblet geometry made during manufacturing, it is hard to believe the full extent of the drag reduction.

The fabric of the swimsuit is knit and the riblet pattern is believed to be embossed. Dean and Bhushan[15] reported that unstretched riblets are tightly packed. As the fabric stretches, the riblet width and spacing increase. The associated decrease in h/s ratio depends on the dimensions of each swimmer's body, which is another compromising factor in the design. Riblet thickness is also a factor considered in the design. Aside from the limitations imposed by the fabrication of patterns available, flexibility in the riblet tips will hinder the fabric's ability to impede the cross-stream translation of streamwise vortices. Thicker riblets are probably needed, used for strength, and cause a decrease in the peak drag reduction capability compared to thinner riblets.

3.3 Summary

Fluid drag in the turbulent boundary layer is in large part due to the effects of the streamwise vortices formed in the fluid closest to the surface. Turbulence and associated momentum transfer in the outer boundary layers is in large part due to the translation, ejection, and twisting of these vortices. Additionally, the vortices also cause high velocities at the surface which create large shear stresses on the surface. Two mechanisms of riblet drag reduction are believed to be dominant. First, riblets impede the translation of the streamwise vortices, which causes a reduction in vortex ejection and outer layer turbulence. Second, riblets lift the vortices off of the surface and reduce the amount of surface area exposed to the high velocity flow. By modifying the velocity distribution, riblets facilitate a net reduction in shear stress at the surface.

Various riblet shapes have been studied for their drag reducing capabilities, but sawtooth, scalloped, and blade riblets are most common. By varying flow properties or riblet geometries, optimization studies have been performed. Drag reduction by riblet surfaces has been shown to be as high as nearly 10% given an optimal geometry of h/s ~0.5 for blade riblets. Commercial applications of riblets include competition swimsuits, which use a thread-based riblet geometry.

4.0 RICE LEAF AND BUTTERFLY WING EFFECT

Bixler and Bhushan[26, 27] reported that rice leaves and butterfly wings combine the desirable shark skin and lotus effects; creating the so-called rice and butterfly wing effect. Scanning electron micrograph (SEM) images in **Fig. 1** (bottom row) show the surface structures of rice leaves and butterfly wings. The hierarchical structures consisting of micropapillae superimposed by waxy nanobumps in rice leaves and microgrooves on shingle-like scale structures in butterfly wings provide superhydrophobicity and low adhesion. The longitudinal grooves with a transverse sinusoidal pattern in rice leaves and aligned shingle-like scales in butterfly wings provide anisotropic flow. This combination of anisotropic flow, superhydrophobicity, and low adhesion is believed to reduce drag, facilitate self-cleaning and provide anti-fouling.

To understand the effects of wettability, the apparent contact angle (CA) and contact angle hysteresis (CAH) were measured with water and oil droplets in air. Measurements were also made with oil droplets underwater. This is useful when considering self-cleaning efficiency of underwater surfaces contacting oil, or vice versa, where superoleophobicity may repel contaminants. Clean surfaces encourage low drag, so therefore self-cleaning is necessary for underwater applications where oil contaminants are present.

Images of the droplets, contact angles, and conceptual mechanisms of water droplets are presented in **Fig. 5a.** Rice leaf and butterfly wing surfaces are superhydrophobic. The enlarged interface of the water droplets on the surfaces show that air pockets are observed with rice leaf and butterfly wing surfaces indicative of Cassie-Baxter regime. Shark skin is an aquatic animal and is superhydrophilic. All three surfaces are superhydrophilic as indicated in **Fig. 5b**. Images of the droplets, contact angles, and conceptual mechanisms of oil droplets in water are presented in **Fig. 5c.** Rice leaf and butterfly wing surfaces exhibit superoleophobicity. With rice leaf, the lower surface tension oil spreads over the higher surface tension hierarchical leaf. With butterfly wing, the oil droplet penetrates into the wing upon contact, likely due to the fragile open lattice microstructure. The shark skin surface is superoleophobic. Water soaks into the skin and combined with the impenetrable dermal denticle microstructures produces superoleophobicity. Such superoleophobicity coupled with low adhesion provides self-cleaning underwater.

To measure drag of the structures, replicas were made by Bixler and Bhushan[26, 27]. They used a rectangular flow channel with replicas and measured pressure drop in water, air and oil fluids. **Figure 6(a)** shows representative data of pressure drop in water both in laminar and turbulent flow for rice leaf and butterfly wings[26]. The data are compared with that for the flat control sample. The pressure drop reduction is calculated from the flat control sample. Pressure drop reduction is observed for both samples with the reduction being larger at higher velocity in the turbulent flow regime.

Figure 6(b) shows the best examples of pressure drop in air, water and oil in turbulent and laminar flow[23, 26, 27]. The data are compared with that for the flat control sample. Selected replica samples were also coated with superhydrophobic and/or superoleophobic coatings to explore their benefits. In air and water flow, pressure drop reduction with superhydrophobic shark skin replica is found to be about 27% and 29%, respectively. In oil flow,

pressure drop reduction with hydrophilic rice leaf replicas and replicas coated with superhydrophobic (superoleophilic) or superoleophobic coatings was about 10%. Mechanisms responsible for pressure drop reduction are different for various replicas[27]. In the case of the superoleophilic replica, pressure drop reduction occurs with a thin oil film leading to reduced skin friction. Whereas, in the case of the superoleophobic replica, pressure drop reduction occurs due to oil repellency and low adhesion.

Bixler and Bhushan[26, 27] have reported data on self-cleaning experiments on various replicas and have shown that rice leaf and butterfly structures exhibit self-cleaning properties.

4.1 Nondimensional pressure drop model

Bixler and Bhushan[27] derived a relationship for nondimensional pressure drop $(\overline{\Delta p})$ as a function of Reynolds number. **Figure 7** shows the plot of $\overline{\Delta p}$ as a function of Reynolds number for a flat hydrophilic closed channel in laminar and turbulent flow. The slope changes between laminar and turbulent flow. The measured pressure drop data in water, oil, and air fluids are also shown in **Fig. 7**. As shown, the nondimensinal pressure drop values follows similar calculated linear trends lines based on water flow. The data shows that nondimensional pressure drop relationship is applicable to fluids with a wide range of densities and viscosities.

4.2 Summary

Rice leaf and butterfly wings combine the desirable shark skin (anisotropic flow leading to low drag) and lotus leaf (superhydrophobic and self-cleaning) effects; creating the so called rice and butterfly wing effect. The rice and butterfly wing effect has been characterized through a series of experiments using both actual and replica samples.

Rice leaf surface is attractive due to its relatively simple two-dimensional micropapillae morphology[24]. Bioinspired surfaces may be created using a dual hierarchical micropattern of cylindrical pillars arranged in longitudinal rows.

5.0 OUTLOOK

The emerging field of biomimetics is already gaining a foothold in the scientific and technical arena. It is clear that nature has evolved and optimized a large number of materials and structured surfaces with rather unique characteristics. Nature capitalizes on hierarchical structure using basic materials to provide functionality of interest. As we understand the underlying mechanisms, we can begin to exploit them for commercial applications. Significant advancements in nanofabrication allow one to replicate structures of interest in biomimetics using smart materials. The commercial applications include nanomaterials, nanodevices, and processes. These include surfaces with superhydrophobicity, self-cleaning, and low or high adhesion, with reversible adhesion, and low drag surfaces, to name a few.

REFERENCES

[1] Bhushan, B., "Biomimetics: Lessons from Nature - An Overview," *Phil. Trans. R. Soc. A* **367**, 1445-1486 (2009).

[2] Bhushan, B., *Biomimetic: Bio-inspired Hierarchical-Structured Surfaces for Green Science and Technology*, Springer-Verlag, Heidelberg, Germany (2012).

[3] Bar-Cohen, Y., *Biomimetics: Nature-Based Innovation*, CRC Press, Boca Raton, FL (2011).

[4] Nosonovsky, M. and Bhushan, B., *Multiscale Dissipative Mechanisms and Hierarchical Surfaces: Friction, Superhydrophobicity, and Biomimetics*, Springer-Verlag, Heidelberg, Germany (2008).

[5] Bhushan, B., *Introduction to Tribology*, 2nd ed. Wiley, NY (2013).

[6] Barthlott, W. and Neinhuis, C., "Purity of the Sacred Lotus, or Escape from Contamination in Biological Surfaces," *Planta* **202,** 1-8 (1997).

[7] Neinhuis, C., and Barthlott, W., "Characterization and Distribution of Water-Repellent, Self-Cleaning Plant Surfaces," *Annals of Botany* **79,** 667-677 (1997).

[8] Bhushan, B. and Jung, Y.C., "Micro and Nanoscale Characterization of Hydrophobic and Hydrophilic Leaf Surface," *Nanotechnology* **17,** 2758-2772 (2006).

[9] Wenzel, R. N., "Resistance of Solid Surfaces to Wetting by Water," *Indust. Eng. Chem*. **28,** 988-994 (1936).

[10] Cassie, A. and Baxter, S., "Wettability of Porous Surfaces," *Trans. Faraday Soc*. **40,** 546-551 (1944).

[11] Jung, Y. C. and Bhushan, B., "Mechanically Durable CNT-Composite Hierarchical Structures with Superhydrophobicity, Self-Cleaning, and Low-Drag," *ACS Nano* **3**, 4155-4163 (2009).

[12] Ebert, D. and Bhushan, B., "Durable Lotus-Effect Surfaces with Hierarchical Structure Using Micro- and Nanosized Hydrophobic Silica Particles," *J. Colloid Interf. Sci.* **368**, 584-591 (2012a).

[13] Ebert, D. and Bhushan, B., "Transparent, Superhydrophobic, and Wear-Resistant Coatings on Glass and Polymer Substrates Using SiO_2, ZnO, and ITO Nanoparticles," *Langmuir* (in review) (2012b).

[14] Choi K.S., Yang X., Clayton B.R., Glover E.J., Altar M., Semenov B.N., and Kulik V.M., "Turbulent Drag Reduction using Compliant Surfaces," *Proc. R. Soc. A* **453**, 2229-2240 (1997).

[15] Dean, B. and Bhushan, B., "Shark-Skin Surfaces for Fluid-Drag Reduction in Turbulent Flow: A Review," *Phil. Trans. R. Soc. A* **368**, 4775-4806 (2010); **368** 5737 (2010).

[16] Bechert D.W., Bruse M., Hage W., Van Der Hoeven J.G.T., and Hoppe G., "Experiments on Drag Reducing Surfaces and Their Optimization with an Adjustable Geometry," *J. Fluid Mech.* **338**, 59-87 (1997).

[17] Kline, S.J., Reynolds W.C., Schraub F.A., and Runstadler P.W., "The Structure of Turbulent Boundary Layers," *J. Fluid Mech.* **30**, 741-773 (1967).

[18] Lee S.-J., and Lee S.-H., "Flow Field Analysis of a Turbulent Boundary Layer Over a Riblet Surface," *Exp. Fluids* **30**, 153-166 (2001).

[19] Bechert, D.W., Bartenwerfer, M., Hoppe, G., and Reif, W.-E., "Drag Reduction Mechanisms Derived from Shark Skin," Paper # ICAS-86-1.8.3, *Proc. 15th ICAS Congress*, Vol. 2 (A86-48-97624-01), pp. 1044-1068, AIAA, New York (1986).

[20] Bechert D.W., Bruse M., and Hage W., "Experiments with Three-Dimensional Riblets as an Idealized Model of Shark Skin," *Exper. Fluids* **28,** 403-412 (2000).

[21] Jung Y.C. and Bhushan, B., "Biomimetic Structures for Fluid Drag Reduction in Laminar and Turbulent Flows," *J. Phys.: Condens. Matt.* **22**, 035104 (2010).

[22] Lang A.W., Motta P., Hidalgo P., and Westcott M., "Bristled Shark Skin: A Microgeometry for Boundary Layer Control?" *Bioinspir. Biomim.* **3**, 1-9 (2008).

[23] Bixler, G.D. and Bhushan, B., "Fluid Drag Reduction with Shark-skin Riblet Inspired Microstructured Surfaces," *Adv. Func. Mater.* (2013).

[24] Bixler, G.D. and Bhushan, B., "Shark Skin Inspired Low-drag Microstructured Surfaces in Closed Channel Flow," *J. Colloid Interf. Sci.* **393**, 384-396 (2013).

[25] Bixler, G.D. and Bhushan, B., "Bioinspired Micro/Nanostructured Surfaces for Oil Drag Reduction in Closed Channel Flow," *Soft Matter* **9**, 1620-1635 (2013).

[26] Bixler, G.D. and Bhushan, B., "Bioinspired Rice Leaf and Butterfly Wing Surface Structures Combining Shark Skin and Lotus Effects," *Soft Matter* **8**, 11271-11284 (2012).

[27] Bixler, G. D. and Bhushan, B., "Fluid Drag Reduction and Efficient Self-Cleaning with Rice Leaf and Butterfly Wing Bioinspired Surfaces," *Nanoscale* (2013).

[28] Bhushan, B., Jung, Y. C., and Koch, K., "Micro-, Nano-, and Hierarchical Structures for Superhydrophobicity, Self Cleaning, and Low Adhesion," *Phil. Trans. R. Soc. A* **367**, 1631-1672 (2009).

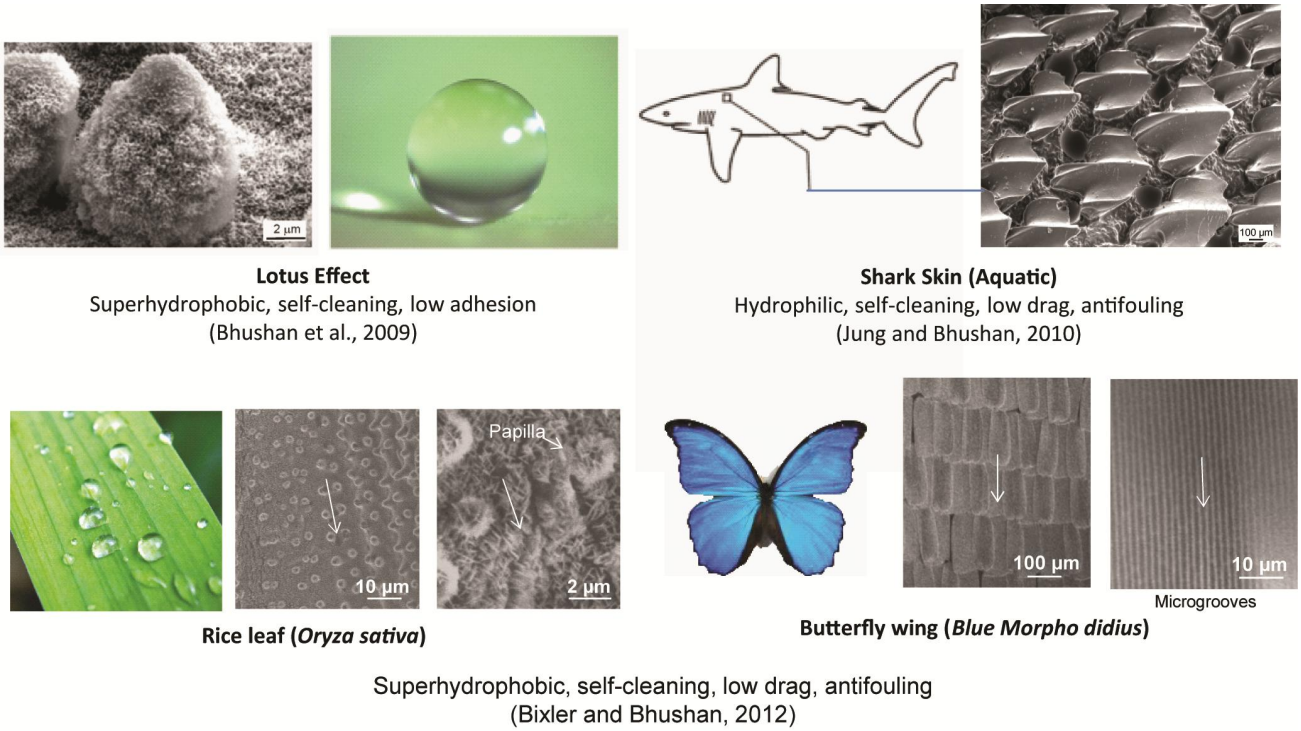

Fig. 1 Montage of four examples from nature

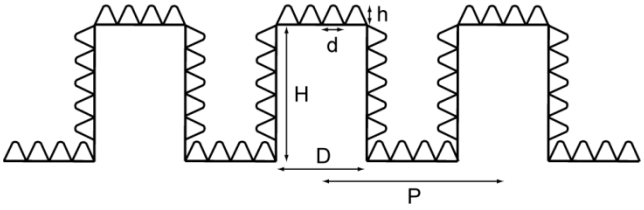

Fig. 2 Schematic of the structure of an ideal hierarchical surface. Microasperities consist of circular pillars with diameter D, height H, and pitch P. Nanoasperities consist of pyramidal nanoasperities of height h and diameter d with rounded tops[28].

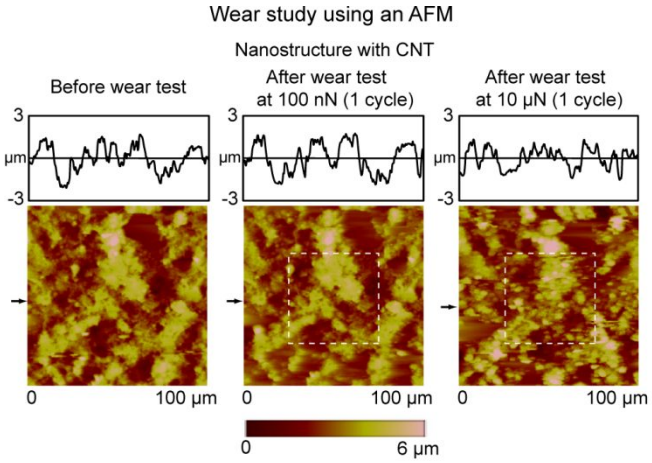

Fig. 3 Surface height maps before and after wear tests with a 15 μm radius borosilicate ball at 100 nN and 10 μN for nanostructures with CNT using an AFM[11].

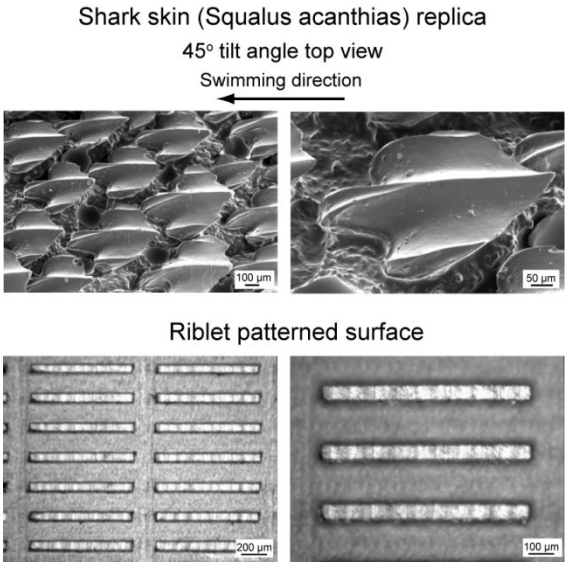

(a)

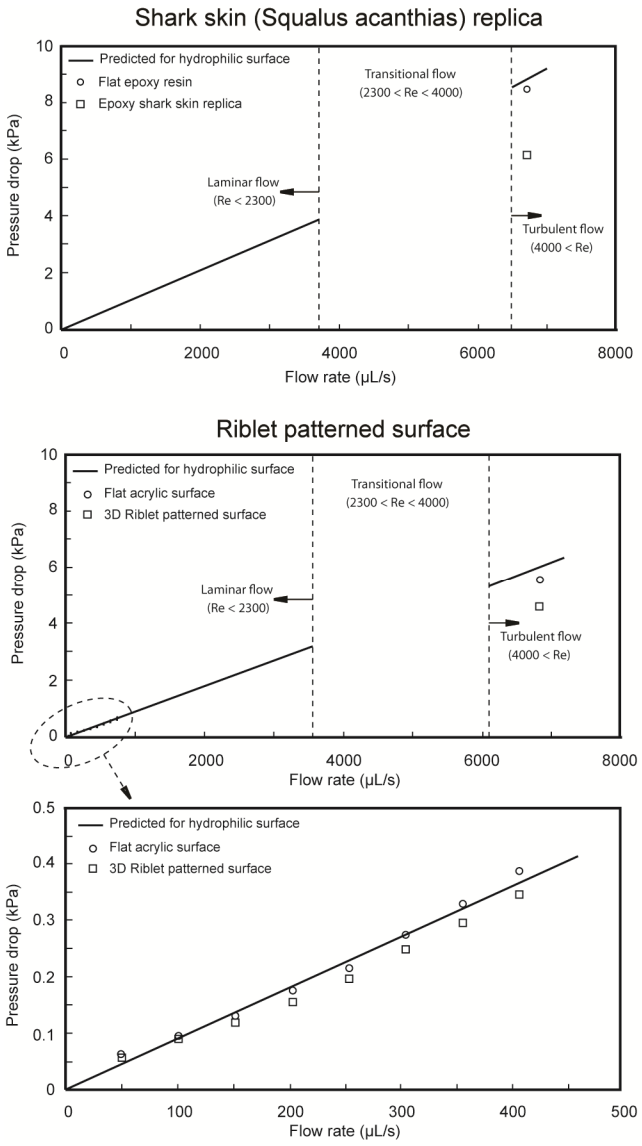

(b)

Fig. 4 (a) SEM micrographs of shark skin replica patterned in epoxy and segmented blade-style riblets fabricated from acrylic, and (b) comparison of pressure drop in a closed rectangular channel flow over a flat epoxy surface and epoxy with shark skin replica surface and over flat acrylic surface and segmented blade riblets. All experiments were performed using water. Data are compared with the predicted pressure drop function for a hydrophilic surface[21].

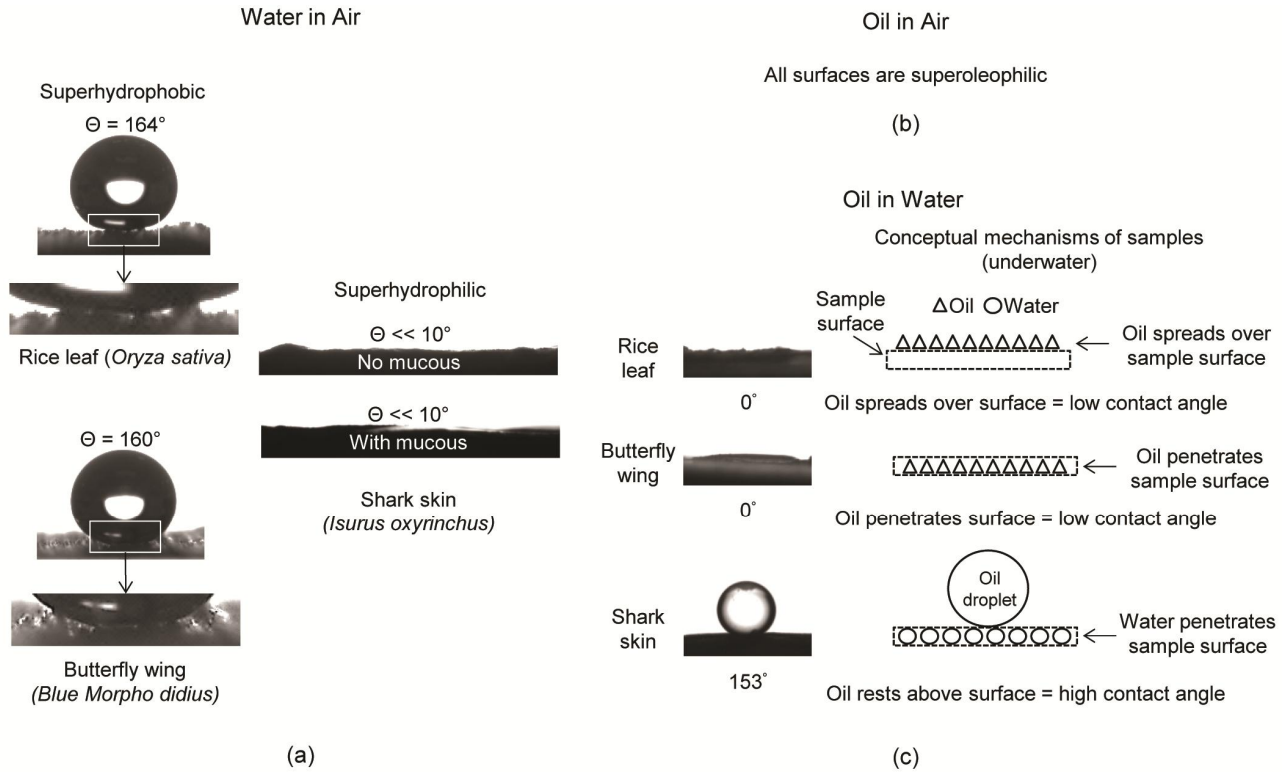

Fig. 5 (a) Water droplet images indicating that rice leaves and butterfly wings are superhydrophobic, whereas shark skin is superhydrophilic, (b) all surfaces were superoleophilic with oil in air, and (c) oil droplet images in underwater indicating that rice leaves and butterfly wings are superoleophilic whereas shark skin is superoleophobic. Nominal apparent contact angle values and conceptual models of mechanisms influencing contact angles are also presented[26].

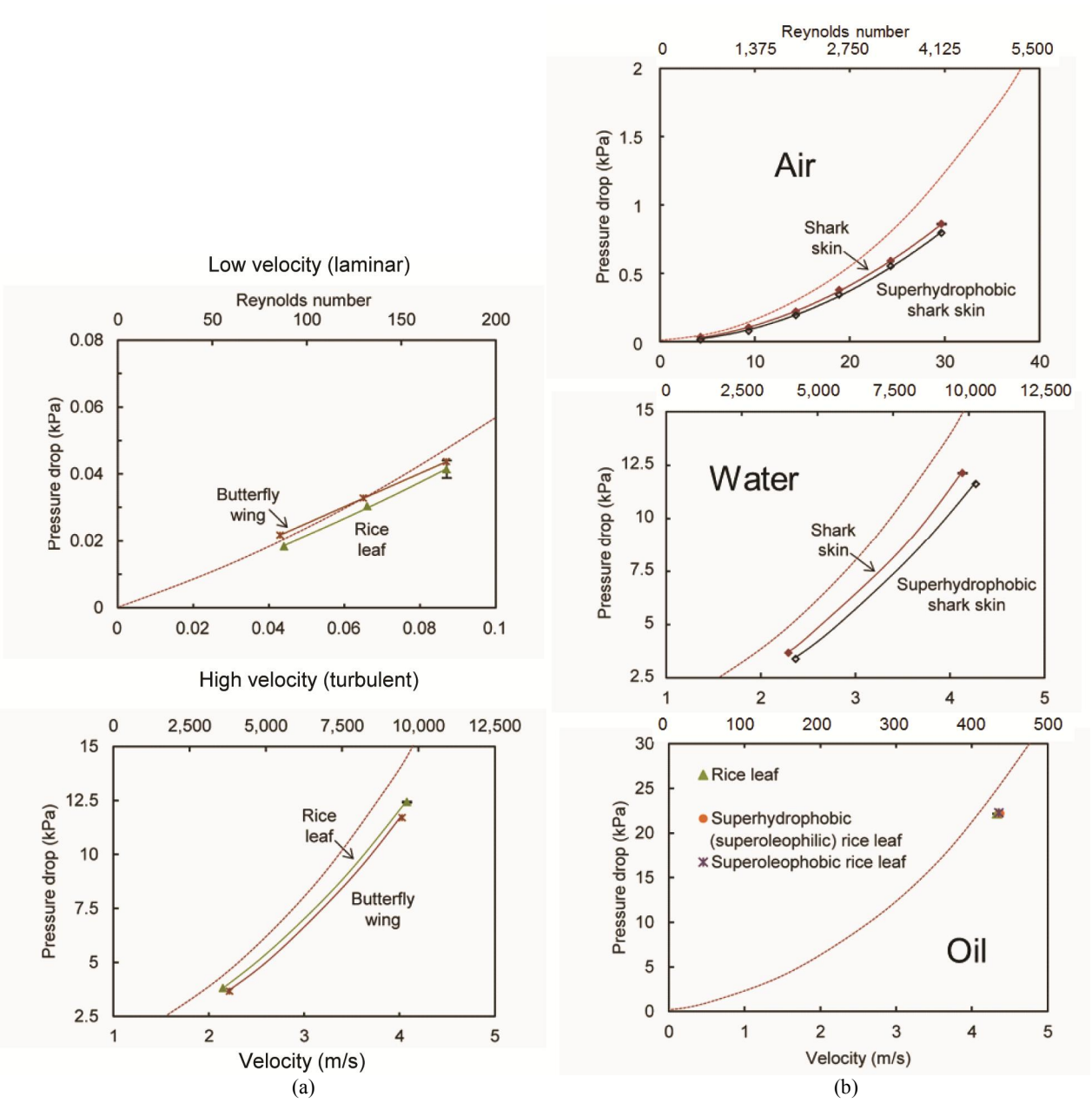

Fig. 6 (a) Water pressure drop with laminar flow and turbulent flow for replicas of rice leaf and butterfly wing surfaces[26], and (b) best example of air, water, and oil pressure drop with turbulent and laminar flow for shark skin and rice leaf surfaces[23, 26, 27]. For comparison, the predicted pressure drop for a flat rectangular closed channel flow is shown. Higher pressure drop translate into higher drag; therefore low pressure drop is desirable. Error bars ±1 standard deviation are hardly visible in the plots.

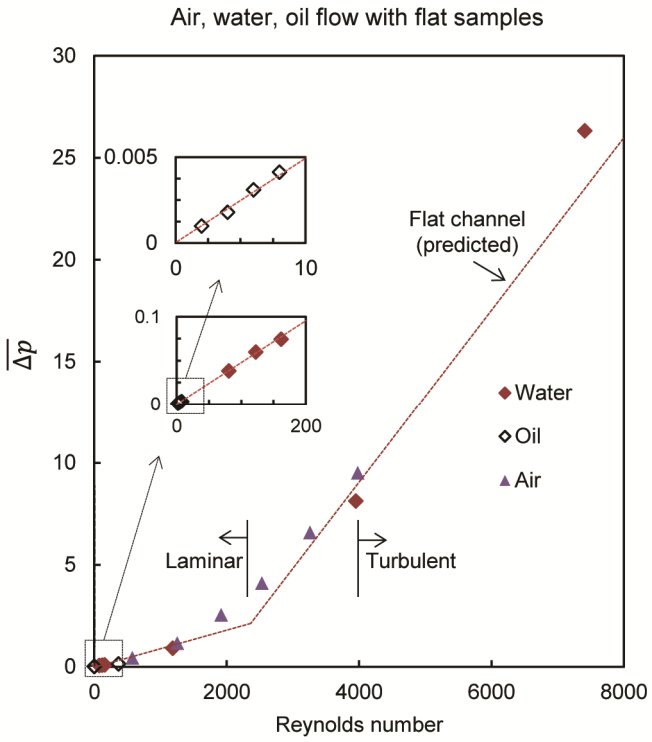

Fig. 7 Predicted nondimensional pressure drop parameter $(\overline{\Delta p})$ as a function of Reynolds number for a flat, hydrophilic closed channel in laminar and turbulent flow. Also presented are data from water, oil, and air experiments[27]. The plot provides flat channel pressure drop estimations based on fluid properties, flow conditions, and channel dimensions.